Diffraction in Charged Current DIS

M. Bertini[a], M. Genovese[b], N.N. Nikolaev[c], B.G. Zakharov[c]

[a] *INFN, Sezione di Torino, Via P.Giuria 1, I-10125 Torino, Italy*

[b] *Istituto Elettrotecnico Nazionale Galileo Ferraris*
Str. delle Caccie 91
10135 Torino, Italy.

[c]*IKP(Theorie), KFA Jülich, 5170 Jülich, Germany*

and L. D. Landau Institute for Theoretical Physics, GSP-1, 117940,
ul. Kosygina 2, Moscow V-334, Russia.

Abstract

We present the QCD calculation of the diffractive structure function for charged current DIS. In particular we analyse the perturbatively tractable excitation of heavy quarks. We emphasize the peculiarities of the Regge factorization breaking in excitation of open charm.

E-mail: kph154@aix.zam.kfa-juelich.de

In the last years successful quantitative predictions for diffractive electromagnetic Deep Inelastic Scattering have been obtained in perturbative QCD (pQCD) [1 - 10]; for a recent review see [11].

In the next future, diffraction in charge current (CC) DIS, $ep \rightarrow \nu p'X$, can shed more light on the pQCD mechanism of Diffractive DIS. Rapidity gap events in CC DIS have already

been observed at HERA [12] and with amassing more data on CC DIS a detailed comparison between the experiment and models for diffractive DIS will be possible [14]. Because of the parity non-conservation, in the CC case one has a larger variety of diffractive SF's compared to the neutral current electromagnetic (EM) case. To the lowest order in pQCD, CC diffractive DIS proceeds by the Cabibbo-favoured excitation of the $(u\bar{d})$ and $(c\bar{s})$ dijet states. The unequal mass for the $(c\bar{s})$ final state is a particularly interesting laboratory for studying the diffractive factorization breaking. A self-tagging property of charm jets gives better access to various diffractive structure functions, for instance, to $F_3^{D(3)}$.

The subject of this paper is the derivation of the above stated features of CC DDIS and its distinction from the EM one. For convenience we focus on the process $e^+ p \to \bar{\nu} p' X$ already observed by ZEUS [12]. The discussion and results being easily translated to the $e^- p \to \nu p' X$ process. In diffractive CC $e^+ p$ scattering the experimentally measured quantity is the five-fold differential cross section $d\sigma^{(5)}(ep \to \nu p' X)/dQ^2 dx dM^2 dp_\perp^2 d\phi$. Here X is the diffractive state of mass M, p' is the secondary proton with the transverse momentum $\vec{p}_\perp$, $t = -\vec{p}_\perp^2$, ϕ is the angle between the (e, e') and (p, p') planes, $Q^2 = -q^2$ is the virtuality of the W^+ boson, $x, y, x_{\mathbf{P}}$ and $\beta = x/x_{\mathbf{P}}$ are the standard diffractive DIS variables.

The underlying subprocess is diffraction excitation of the W^+ boson, $W^+ p \to p' X$. In the parity conserving EM DIS, the exchanged photon have either longitudinal (scalar), $s = \frac{1}{Q}(q_+ n_+ - q_- n_-)$ or transverse, in the (e, e') plane, polarization t_μ (here $n_\pm$ are the usual lightcone vectors, $n_+^2 = n_-^2 = 0$, $n_+ n_- = 1$, $q = q_+ n_+ + q_- n_-$ and $q.s = q.t = 0$). In the parity-nonconserving CC DIS, the exchanged W^+ bosons have also the out-of-plane linear polarization $w_\mu = \epsilon_{\mu\nu\rho\sigma} t_\nu n_\rho^+ n_\sigma^-$. We introduce also the usual transverse metric tensor $\delta_{\mu\nu}^\perp = \delta_{\mu\nu} + n_\mu^- n_\nu^+ + n_\mu^+ n_\nu^- = -t_\mu t_\nu - w_\mu w_\nu$. Then, the polarization state of the W^+ is described by the leptonic tensor

$$L_{\mu\nu} = \frac{2Q^2}{y^2} \left[-\frac{1}{2}\delta_{\mu\nu}^\perp (1 - y + \frac{1}{2}y^2) + \frac{1}{2}(1 - y)(t_\mu t_\nu - w_\mu w_\nu) + (1 - y)s_\mu s_\nu \right.$$
$$\left. +\frac{1}{2}(1 - \frac{1}{2}y)\sqrt{1 - y}(s_\mu t_\nu + s_\nu t_\mu) + \frac{i}{2}y(1 - \frac{1}{2}y)(w_\mu t_\nu - w_\nu t_\mu) + \frac{i}{2}y\sqrt{1 - y}(w_\mu s_\nu - s_\mu w_\nu) \right] \quad (1)$$

which, upon contraction with the hadronic tensor leads to 6 different components for $d\sigma_i^{(3)}(W^+ p \to p' X)/dM^2 dt d\phi$ labeled by $i = T, L, TT', LT, 3$ and $LT(3)$:

2

$$y \frac{d\sigma^{(5)}(e^+p \to \bar{\nu}p'X)}{dQ^2 dy dM^2 dp_\perp^2 d\phi} = \frac{G_F M_W^2 Q^2}{4\sqrt{2}\pi^2(M_W^2 + Q^2)^2} \left\{ (1 - y + \frac{1}{2}y^2) \cdot d\sigma_T^{D(3)} - y(1 - \frac{1}{2}y) \cdot d\sigma_3^{D(3)} \right.$$

$$+ (1 - y) \cdot d\sigma_L^{D(3)} + (1 - y)\cos 2\phi \cdot d\sigma_{TT'}^{D(3)}$$

$$\left. + (1 - \frac{1}{2}y)\sqrt{1 - y}\cos\phi \cdot d\sigma_{LT}^{D(3)} - y\sqrt{1 - y}\sin\phi \cdot d\sigma_{LT(3)}^{D(3)} \right\} / dM^2 dp_\perp^2 d\phi \,, \quad (2)$$

where G_F is the Fermi coupling, M_W is the mass of the W-boson. Each and every $d\sigma_i^{(3)}(W^+p \to p'X)$ defines a set of dimensionless diffractive structure functions $F_i^{D(4)}$:

$$(Q^2 + M^2) \frac{d\sigma_i^{(3)}(W^+p \to p'X)}{dM^2 dp_\perp^2} = \frac{\pi G_F M_W^2 Q^2}{\sqrt{2}(Q^2 + M_W^2)^2} \cdot \frac{\sigma_{tot}^{pp}}{16\pi} \cdot F_i^{D(4)}(p_\perp^2, x_{\mathbb{P}}, \beta, Q^2) \,, \quad (3)$$

It is also useful to introduce the t-integrated SF's [1]

$$F_i^{D(3)}(x_{\mathbb{P}}, \beta, Q^2) = \frac{\sigma_{tot}^{pp}}{16\pi} \int dp_\perp^2 F_i^{D(4)}(p_\perp^2, x_{\mathbb{P}}, \beta, Q^2) \,. \quad (4)$$

The diffractive SF's $F_T^{D(3)}, F_L^{D(3)}$ and $F_3^{D(3)}$ are counterparts of the familar $F_T = F_2 - F_L, F_L$ and F_3 for inclusive DIS of neutrinos, $F_3^{D(3)}$ and $F_{LT(3)}^{D(3)}$, are C- and P-odd and vanish in EM scattering. The discussion of the azimuthal angle-dependent terms TT', LT and $LT(3)$ goes beyond the scope of this letter, in which we focus on $F_T^{D(3)}, F_L^{D(3)}$ and $F_3^{D(3)}$.

Up to now only relatively large $x \sim 10^{-2}$ are easily accessible in CC DIS [12, 14]. As for selecting diffractive events, one requires $x_{\mathbb{P}} <$ (0.05-0.1), the kinematical relation $\beta = x/x_{\mathbb{P}}$ implies that the experimentally observed CC diffractive DIS will proceed at rather large β, dominated by the partonic subprocess $W^+p \to (u\bar{d})p', (c\bar{s})p'$. The relevant pQCD diagrams are shown in Fig. 1. In the following, we focus on the $c\bar{s}$ excitation, analogous considerations apply to $u\bar{d}$. z and $(1-z)$ are the fractions of the (light–cone) momentum of the W^+ carried by the charmed quark and strange antiquark respectively, $\vec{k}$ is the relative transverse momentum in the $q\bar{q}$ pair (Fig. 1). The invariant mass of the dijet final states equals

$$M^2 = \frac{k^2 + \mu^2}{z(1 - z)} \,, \quad (5)$$

---

[1]Our definition (4) of $F_i^{D(3)}$ differs from the ZEUS/H1 [13] by the factor $x_{\mathbb{P}}$, so that $F_i^{D(3)}$ does not blow up at $x_{\mathbb{P}} \to 0$

where $\mu^2 = (1 - z)m_c^2 + zm_s^2$. m_c, (m_s) being the charmed (strange) quark mass. All SF's are calculable in terms of the same quark helicity changing and conserving amplitudes $\vec{\Phi}_1$ and Φ_2 introduced in [1, 2]. Combining the formalism of [2] with the treatment of charm leptoproduction in [15], we have obtained (integration over the azimuthal orientation of $\vec{k}$ is understood, $\alpha_{cc} = \frac{G_F M_W^2}{2\pi\sqrt{2}}$)

$$\frac{d\sigma_{L,T}^D}{dzdk^2dt}\Big|_{t=0} = \frac{\pi^2\alpha_{cc}}{3}\alpha_S^2(\bar{Q}^2)\left[A_{L,T}(z, m_s, m_c)\vec{\Phi}_1^2 + B_{L,T}(z, m_s, m_c)\Phi_2^2\right], \quad (6)$$

where

$$A_T(z) = [1 - 2z(1 - z)], \quad (7)$$

$$B_T(z, m_s, m_c) = \left[m_c^2 - 2z(1 - z)m_c^2 - z^2\Delta^2\right], \quad (8)$$

$$A_3(z) = [2z - 1], \quad (9)$$

$$B_3(z, m_s, m_c) = \left[z^2 m_s^2 - (1 - z)^2 m_c^2\right], \quad (10)$$

$$A_L(z, m_s, m_c) = \frac{1}{Q^2}(m_s^2 + m_c^2), \quad (11)$$

$$B_L(z, m_s, m_c) = 4Q^2z^2(1 - z)^2 + 4z(1 - z)\mu^2 + \frac{1}{Q^2}[\mu^4 + m_c^2 m_s^2] \quad (12)$$

with $\Delta^2 = m_c^2 - m_s^2$. The amplitudes $\vec{\Phi}_1$ and Φ_2 were derived in [1, 2] and, to a logarithmic accuracy,

$$\vec{\Phi}_1 \approx 2\vec{k}(1 - \beta)^2\frac{[(k^2 + \mu^2)\beta + (1 - \beta)\mu^2]}{(k^2 + \mu^2)^3}\int\frac{d\tau}{\tau}W_1(\omega, \tau)G(x_{\mathbb{P}}, \tau\bar{Q}^2) \quad (13)$$

$$\Phi_2 \approx (1 - \beta)^2\frac{[(k^2 + \mu^2)(1 - 2\beta) - 2\beta\mu^2]}{(k^2 + \mu^2)^3}\int\frac{d\tau}{\tau}W_2(\omega, \tau)G(x_{\mathbb{P}}, \tau\bar{Q}^2) \quad (14)$$

where $G(x, Q^2) = xg(x, Q^2)$ is the gluon distribution in the proton and $\varepsilon^2 = z(1 - z)Q^2 + \mu^2$. As in the EM case [6, 7, 9, 10] the relevant effective pQCD factorization scale is found to be

$$\bar{Q}^2 = \varepsilon^2 + k^2 = \frac{k^2 + \mu^2}{(1 - \beta)} \quad (15)$$

and has already been used in (6) as the argument of strong coupling α_S.

Here the weight functions $W_i(\omega = k^2/\varepsilon^2, \tau = \kappa^2/\bar{Q}^2)$ have a narrow peak at $\tau \approx 1$ with the unit area under the peak, which gives the Leading LogQ^2 result [2, 6, 8]

4

$$\int \frac{d\tau}{\tau} W_i(\omega, \tau) G(x_{\mathbb{P}}, \tau \bar{Q}^2) \approx G(x_{\mathbb{P}}, \bar{Q}^2), \tag{16}$$

valid for sufficiently large values of ω, which is equivalent to sufficiently large $\beta \gtrsim 0.1$ of the interest in the present study.

At variance with the equal mass EM case, where $\bar{Q}^2 = (k^2 + m^2)/(1 - \beta)$, now the factorization scale depends on z and then one expects different cross sections whether the charmed quark is produced in the forward (F) or the backward (B) hemisphere, with respect to the W momentum, in the rest frame of the diffractive state X. The two configurations differ by the value of the light-cone variable $z_{F,B} = \frac{1}{2}(1 + \delta)\left[1 \pm \sqrt{1 - 4\frac{k^2 + m_c^2}{M^2(1+\delta)^2}}\right]$, where $\delta = \frac{\Delta^2}{Q^2} \frac{\beta}{(1-\beta)}$. The pQCD scale is perturbatively large for large β even for light flavours, and for the charm component of the diffractive SF it is large for all β, see below.

To evaluate the light quark component of the diffractive SF at not really large β, one needs a model for the small-Q^2 behaviour of the gluon structure function $G(x, Q^2)$: in the following we will use the same form used in Ref. [8], which at large Q^2 coincide with the GRV NLO parameterization [19]. Furthermore we take $m_c = 1.5$ GeV, $m_s = 0.3$ GeV and $m_{u,d} = 150$ MeV. Variations of the charm mass by 10% have a small effect on the predicted SF, apart from shifting the threshold $\beta_c = Q^2/[Q^2 + (m_c + m_s)^2]$ (see below).

In the evaluation of $F_i^{D(3)}$ one needs to know the $p_\perp^2$ dependence of the diffractive cross section, which is usually parameterized as $d\sigma/dp_\perp^2 \propto \exp(-B_D p_\perp^2)$. As it was shown in [17, 11], one can use $B_D \sim 6$ GeV^{-2} for heavy flavour excitation and for the perturbative transverse higher twist and logitudinal contributions while for light flavour contribution the diffraction slope B_D exhibits, at not so large β, a slight β-dependence, but for the purposes of this present exploratory study we shall simply take $B_D(ud) \sim 9$ GeV^{-2}.

Many authors treats diffractive DIS as DIS off pomerons in the proton, assuming implicitly and explicitly the diffractive factorization. The latter is not supported by QCD studies [4, 6], and the present study of charm excitation in CC diffractive DIS offers more evidence to this effect. Still it is not confusing, we shall speak of the perturbative intrinsic partons in the pomeron.

Separation of the pQCD subprocess of $W^+ \to c\bar{s}$ into the excitation of charm on the

perturbative intrinsic strangeness in the pomeron and excitation of (anti)strangeness on the intrinsic (anti)charm is not unambiguous and must be taken with the grain of salt. In the naive parton model, in the former process charmed quark will carry the whole momentum of the W^+ and be produced with $z \approx 1$. In contrast, in the latter process, it is the strange antiquark which carries the whole momentum of W^+ and charmed quark is produced with $z \approx 0$, which suggests $z > \frac{1}{2}$ and $z < \frac{1}{2}$ as a compromise boundary between the two partonic subprocesses. However, the full fledged pQCD calculation leads to broad z distributions (for a related discussion of definition of the strangeness and charm density in $\nu N, \bar{\nu} N$ inclusive DIS see [15]). As a purely operational definition, we stick to a parton model decomposition $F_T^{D(3)}(c\bar{s}) = F_{T(s)}^{D(3)} + F_{T(\bar{c})}^{D(3)}$ and $F_3^{D(3)}(c\bar{s}) = F_{T(s)}^{D(3)} - F_{T(\bar{c})}^{D(3)}$, which is a basis for the results shown in Fig. 2. With this definition, excitation of the charmed quark off the intrinsic strangeness, $F_{T(s)}^{D(3)}$, comes from terms $\propto z^2$ in (7, 8) and (9, 10). It is dominated by the forward production of charm w.r.t. the momentum of W^+ in the rest frame of the diffractive system X, but receives certain contribution also from $z < \frac{1}{2}$. Similarly, $F_{T(\bar{c})}^{D(3)}$ some from terms $\propto (1-z)^2$, is dominated by the forward production of strangeness (the backward production of charm), but still receives certain contribution from the forward charm production.

All the considerations of Ref. [7, 8] for the longitudinal and transverse diffractive SF in electroproduction are fully applicable to the CC case at $Q^2 \gg m_c^2$. We consider first the backward charm, $z \ll 1$, for which Eq.s (5, 15) give $z \approx (k^2 + \mu^2)/M^2$ and $\bar{Q}^2 \approx (k^2 + m_c^2)/(1 - \beta)$. Expanding the brackets of Eqs.(13, 14), in Eq.(6) and using the approximation (16) the k^2-integration in (6) gives dominant contributions to the transverse SF coming from the low-k^2 region but without entering deeply in the nonperturbative region for the heavy quark production. For $M^2 \gg m_c^2$ one finds for the low scales dominated contribution (including the Leading Twist and the first Higher Twist) :

$$
\begin{aligned}
F_{T(\bar{c})}^{D(4)} &\approx \frac{4\pi}{3\sigma_{tot}^{pp}} \frac{\beta(1-\beta)^2}{6m_c^2(1+\delta)} \left\{ (3 + 4\beta + 8\beta^2) + \frac{m_c^2}{Q^2} \frac{4\beta}{1-\beta} \right. \\
&\left. \times \left[\frac{5}{4} \frac{\Delta^2}{m_c^2}(1 + 8\beta^2) - (1 - 2\beta + 4\beta^2) \right] \right\} \left[\alpha_S(\bar{Q}_L^2) G(x_{\mathbf{P}}, \bar{Q}_L^2 \simeq \frac{m_c^2}{(1-\beta)}) \right]^2
\end{aligned}
\tag{17}
$$

As in the EM case the large k^2 ($k^2 \sim M^2/4$) dominated contributions come from the

6

second term in (7). They are calculable in pQCD and the twist expansion starts with twist-4:

$$F_{T(\bar{c})}^{D(4)} = -\frac{16\pi}{\sigma_{tot}^{pp}} \frac{2}{3} \frac{\bar{\beta}^2(1-\beta)}{Q^2(1+\delta)} \left(\beta^2 + 2\frac{\Delta^2}{Q^2} \frac{\beta^2(2\beta-1)}{(1-\beta)}\right) \left[\alpha_S(\bar{Q}_H^2)G(x_{\mathbb{P}}, \bar{Q}_H^2 \simeq \frac{Q^2}{4\beta})\right]^2 \quad (18)$$

In (17, 18) emerge additional higher-twist corrections $\propto (\Delta^2/Q^2)^n$, in a first approach we restrict ourselves to the leading twist and its first higher twist corrections.

Thus, the higher twist corrections to F_T^D receive contributions both from the low-scale region and the large scale $\bar{Q}_H^2$. The first term in Eq.(18) is substantially the same which has been discussed in Ref. [8] for EM current and it remains relevant even at relatively large value of Q^2 as the $1/Q^2$ factor is partially compensated by the growth of $G(x_{\mathbb{P}}, \bar{Q}_H^2)$.

For what concerns the longitudinal cross section, the most important contribution comes from the term $z^2(1-z)^2Q^2$ in the B_L expansion (12), which is identical to that in the EM case. The k^2 integrated cross section is completely dominated by the short-distance contribution from high-k^2 jets, $k^2 \sim \frac{1}{4}M^2$. Upon the k^2 integration, to a logarithmic accuracy, we find the twist expansion of the longitudinal SF for the terms dominated by the large scale:

$$F_{L(\bar{c})}^{D(4)} = \frac{16\pi}{\sigma_{tot}^{pp}} \frac{\beta^3 (2\beta-1)}{3 Q^2(1+\delta)} \left((2\beta-1) + \frac{\Delta^2}{Q^2} \frac{\beta(5-6\beta)}{(1-\beta)}\right) \left[\alpha_S(\bar{Q}_H^2)G(x_{\mathbb{P}}, \bar{Q}_H^2)\right]^2 \quad (19)$$

As the pQCD scale $\bar{Q}_H^2$ does not depend on flavours we predict a restoration of the flavour symmetry and equal $c\bar{s}$ and $u\bar{d}$ when twist-6 is negligible. Such an equal contribution of light and heavy flavours into the higher twist is unprecedented in the standard inclusive DIS. Again the scaling violation factor $G^2(x_{\mathbb{P}}, \bar{Q}^2)$, in (19), largely compensates the higher twist factor $\frac{1}{Q^2}$ and the longitudinal SF remains large, and takes over F_T^D, in a broad range of Q^2 of practical interest, see Fig. 2.

In (19), the leading twist-4 term is the same as for NC diffractive DIS. However, in the CC diffractive DIS, because non-conservation of weak current, extra higher twist contributions to $F_L^{D(3)}$ come from the expansion of B_L (always substantially dominated by the perturbative region).

Further terms (both twist-4 and higher), come from the term $\propto A_L$ in (6). They receive large contributions from the low k^2 region. In particular they assume a strong relevance for the charm–strange component where terms $\propto m_c^2/Q^2$ appear. We find for the A_L contribution:

$$F_{L(\bar{c})}^{D(4)}[A_L] \approx \frac{4\pi}{9\,\sigma_{tot}^{pp}} \frac{(m_c^2 + m_s^2)}{m_c^2} \frac{\beta(1-\beta)^2}{Q^2(1-\delta)}(1 + 2\beta + 3\beta^2)\left[\alpha_S(\bar{Q}_L^2)G(x_{\mathbb{P}}, \bar{Q}_L^2)\right]^2 \tag{20}$$

Whereas this comtribution is low scale dominated it is comparable to the leading twist-4 in the small Q^2 region. Due to the symmetry $z, (1-z)$ of Eqs.(5, 7 - 12), one finds similar results subject to the replacement $m_c \to m_s$ for the forward production of charm $(F_{(s)}^D)$ at $1 - z \lesssim m_s^2/m_c^2$. The overall dependence of $F_L^{D(3)}(cs)$ on Q^2 and its decomposition in the A_L and B_L components are shown in Fig. 3.

It is interesting to notice that the pQCD scales $\bar{Q}^2(c)$ and $\bar{Q}^2(s)$ are different, both explicitly depend on β, and the $x_{\mathbb{P}}$ and β dependences of $F_{T(i)}^{D(3)}$ are inextricably entangled. This gives another example where the Ingelman-Schlein factorization hypothesis, $F_2^{D(3)}(x_{\mathbb{P}}, \beta, Q^2) = f_{\mathbb{P}}(x_{\mathbb{P}})F_{2\mathbb{P}}(\beta, Q^2)$, with process independent flux of pomerons in the proton $f_{\mathbb{P}}(x_{\mathbb{P}})$ and the $x_{\mathbb{P}}$ independent pomeron SF $F_{2\mathbb{P}}(\beta, Q^2)$, is not confirmed by pQCD calculation. The diffractive factorization breaking in CC diffractive DIS is especially severe, because for the same $c\bar{s}$ final state the pQCD factorization scale $\bar{Q}^2$ changes substantially from the forward to backward hemisphere: $\bar{Q}(s)^2 \ll \bar{Q}(c)^2$. Although the perturbative intrinsic charm component $F_{T(\bar{c})}^{D(3)}$ is suppressed by the mass of a heavy quark, it is still substantial and it is predicted to rise much steeper than the strange one as $x_{\mathbb{P}} \to 0$. Furthermore, $F_{T(\bar{c})}^{D(3)}$ is truly of perturbative origin at all β, while $F_{T(s)}^{D(3)}$ has a non-negligible dependence to small scales up to $\beta \gtrsim 0.7$.

As an illustration of the diffractive factorization breaking, in Fig. 4 we show the effective exponent of the $x_{\mathbb{P}}$ dependence

$$n_{eff} = 1 - \frac{\partial \log F_2^{D(3)}}{\partial \log x_{\mathbb{P}}} \tag{21}$$

evaluated for $x_{\mathbb{P}} = 3 \cdot 10^{-3}$. We show the β dependence of n_{eff} evaluated for $F_2^{D(3)}(u\bar{d} + c\bar{s})$ and $F_2^{D(3)}(u\bar{d})$ for $\beta > 0.2$. At smaller β one expects a further increasing due to the triple pomeron component, see [5].

Evidently, at fixed β, the $c\bar{s}$ excitation is possible only for sufficiently large Q^2 such that $\beta_c > \beta$. For this reason, diffractive SF's exhibit strong threshold effects shown in Fig. 5, which are much stronger than in the NC case studied in [6, 8]. Notice, that $F_3^{D(3)}$ vanishes below the $c\bar{s}$ threshold.

Naively, one would expect $F_3^{D(3)} = 0$ for a quark-antiquark symmetric target as the Pomeron is. Indeed, because $A_3(z)$, and for equal mass case, $B_3(z)$ too, are antisymmetric about $z = \frac{1}{2}$, the contribution from $u\bar{d}$ excitation to $F_3^{D(3)}$ vanishes upon the integration over the u-jet production angles. On the other hand, in the $c\bar{s}$ excitation there is a strong forward-backward asymmetry and $F_3^{D(3)}(c\bar{s}) \neq 0$. Our predictions for $F_3^{D(3)}$ are shown in Fig. 2.

Finally, some comments on the so-called triple-pomeron region, of $\beta \ll 1$, are in order. Here diffraction proceeds via excitation of the soft gluon-containing $q\bar{q}g$ and higher Fock states of the photon. As it has been discussed to great detail in [3, 4], at $\beta \ll 1$ and only at $\beta \ll 1$, and with certain reservations, one can apply the standard parton model treatment to diffractive DIS. For instance, the conventional fusion of virtual photons with the gluon from the two-gluon valence state of the pomeron becomes the driving term of diffractive DIS.

In this case the results for the diffractive SF of light quarks coincide (once the opportune couplings of weak interaction are substituted to the EM ones) with those presented in Ref. [4]. For the charm–strange component it must be considered that now the charm quark is always produced together with a strange one, this leads to a threshold ($Q_{cs}^2 = 4GeV^2$), which is intermediate between the strange ($Q_{ss}^2 = 1GeV^2$) and the charm ($Q_{cc}^2 = 10GeV^2$) electromagnetic DIS thresholds in analogy to our discussion concerning the inclusive DIS [15, 20]; using the the notation of [4] we find $A_{cs} = 0.08$.

Summary and Conclusions.

We have presented the calculation of diffractive structure functions in the QCD color-dipole scheme for charged current DIS and carried on a comparison of diffraction in charged current and electromagnetic DIS. Both charged current and electromagnetic diffraction share the property of diffractive factorization breaking. For instance, we find different $x_{\mathbb{P}}$ dependences of the intrinsic u, d, strangeness and charm composition of the pomeron. Futhermore, we predict a different $x_{\mathbb{P}}$ dependence even for the production of charm quark in the forward and backward direction.

Compared to the EM case, other new features of CC diffraction are the emergence of substantial $F_3^{D(3)}$, and the large higher twist contributions to the longitudinal structure function

because of the non-conservation of weak currents. These predictions will be tested with the accumulation of more data on CC diffraction at HERA and will permit further test of the color dipole picture of DDIS.

References

[1] N.N. Nikolaev and B.G. Zakharov, *Z. Phys.* **C53**, 331 (1992).

[2] N.N. Nikolaev and B.G.Zakharov, *Phys. Lett.* **B332**, 177 (1994).

[3] N.N. Nikolaev and B.G.Zakharov, *JETP* **78**, 598 (1994); *Z. Phys.* **C64** (1994) 631.

[4] M. Genovese, N.N. Nikolaev and B.G. Zakharov, *JETP* **81** 625 (1995).

[5] M. Genovese, N.N. Nikolaev and B.G. Zakharov, *JETP* **81**, 633 (1995).

[6] M. Genovese M., N.N. Nikolaev and B.G. Zakharov, *Phys. Lett.* **B378**, 347 (1996).

[7] M. Genovese, N.N. Nikolaev and B.G. Zakharov, *Phys.Lett.* **B380**, 213 (1996).

[8] M. Bertini, M. Genovese, N.N. Nikolaev, A.V. Pronyaev and B.G. Zakharov, *Phys. Lett.* **B422** (1998) 238.

[9] J. Bartels, J. Ellis, H. Kowalski and M. Wuesthoff hep-ph/9803497, J. Bartels, H. Lotter and M. Wüsthoff, *Phys. Lett.* **B379** (1996) 239, H. Lotter, *Phys. Lett.* **B406** (1997) 171.

[10] E.M. Levin, A.D. Martin, M.G. Ryskin and T. Teubner, *Z. Phys.* **C74** (1997) 671. E.Gotsman, E.Levin and U.Maor, *Nucl. Phys.* **B493** (1997) 354.

[11] Nikolaev N.N. and B.G.Zakharov, Phenomenology of Diffractive DIS. Overview at DIS'97, Chicago, April 97, hep-ph/9706343; M. Genovese, to be published in Proc. of DIS98, Bruxelles, April 98, hep-ph/9805504.

[12] ZEUS Collab., M. Derrick et al., Z. Phys. C72 (1996) 47.

[13] H1 Coll., C. Adloff et al. *Z. Phys.* **C76** (1997) 613,

ZEUS Coll., M. Derrick et al. *Z. Phys.* **C68** (1995) 569.

[14] J. Pliszka and A. F. Zarnecki, Proc. Workshop on Future Physics at HERA (Hamburg 1996) ed. G. Ingelman *et al.*, p728.

[15] V. Barone, M. Genovese, N.N. Nikolaev, E. Predazzi and B.G. Zakharov, Phys. Lett. B328 (1994) 143.

[16] W. Buchmüller, M.F. McDermott and A. Hebecker, hep-ph/9703314.

[17] N.N. Nikolaev, A. Pronyaev and B.G. Zakharov, paper in preparation.

[18] V. Barone et al., *Phys. Lett.* **B292**, 181 (1992). V. Barone, M. Genovese, N.N. Nikolaev, E. Predazzi and B.G. Zakharov, *Int. J. Mod. Phys.* **A8** (1993) 2779.

[19] M. Glück, E. Reya and A. Vogt, *Z. Phys.* **C67**, 433 (1995).

[20] V. Barone, M. Genovese, N.N. Nikolaev, E. Predazzi and B.G. Zakharov, Z. Phys. C70 (1996) 83; Phys. Lett. B304 (1993) 176, B268 (1991) 279, B317 (1993) 433 ; V. Barone and M. Genovese, Phys. Lett. B379 (1996) 233.

Figures
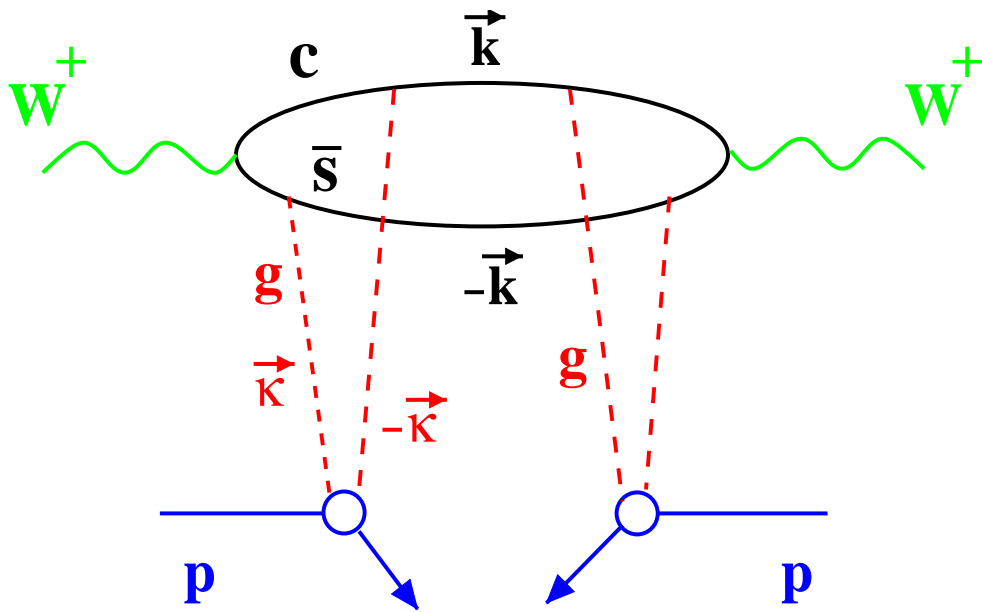
Figure 1: The pQCD Feynman diagrams for diffraction exitation of $c\bar{s}$ $(u\bar{d})$ states of the W.
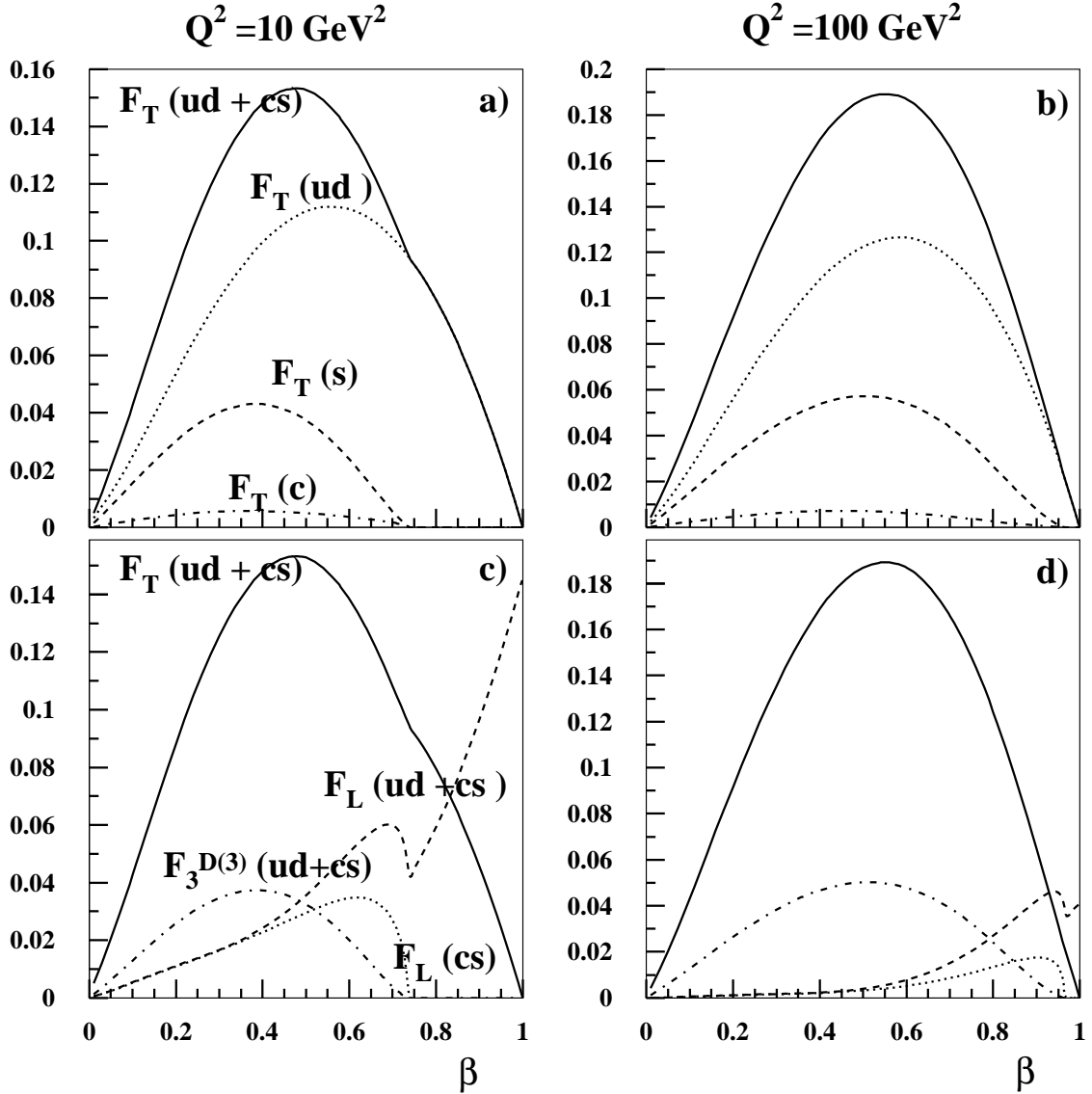
Figure 2: The β dependence for $x_{\mathbb{P}} = 10^{-3}$ of   **a)** $F_T(ud+sc)$ [solid], $F_T(ud)$ [dotted], $F_T(s)$ [dashed], $F_T(c)$ [dot–dashed] at $Q^2 = 10$ GeV^2 **b)** the same as above for $Q^2 = 100$ GeV^2 **c)** All flavours F_T [solid], F_3 [dot–dashed], F_L [dashed] and $F_L(cs)$ [dotted] at $Q^2 = 10$ GeV^2 **d)** the same as above for $Q^2 = 100$ GeV^2
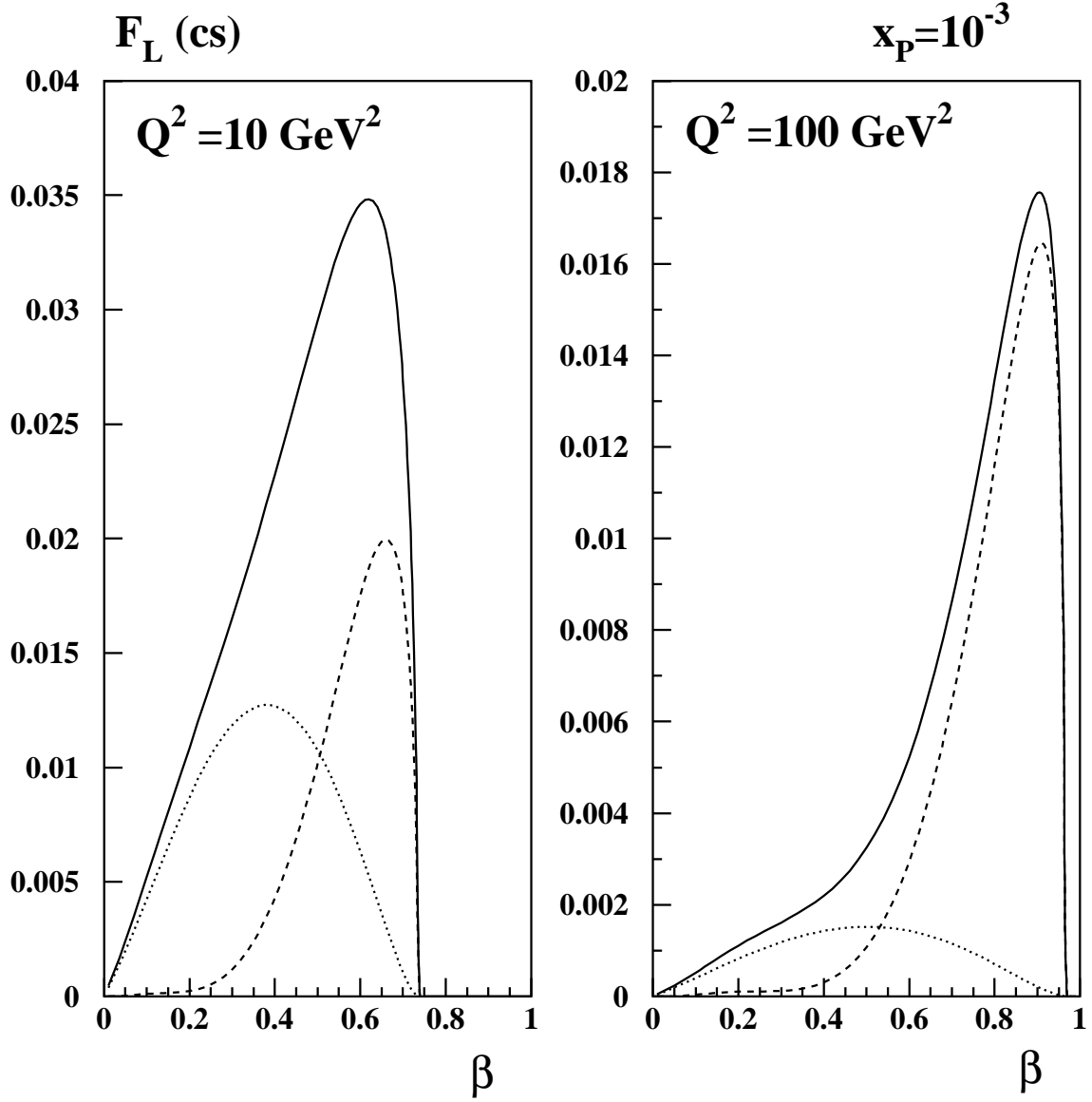
Figure 3: $F_L^{D(3)}(cs)$ [solid] and A_L Eq.(20), [dotted] and B_L Eq.(19), [dot–dashed] components of F_L at Q^2=10,100 GeV².
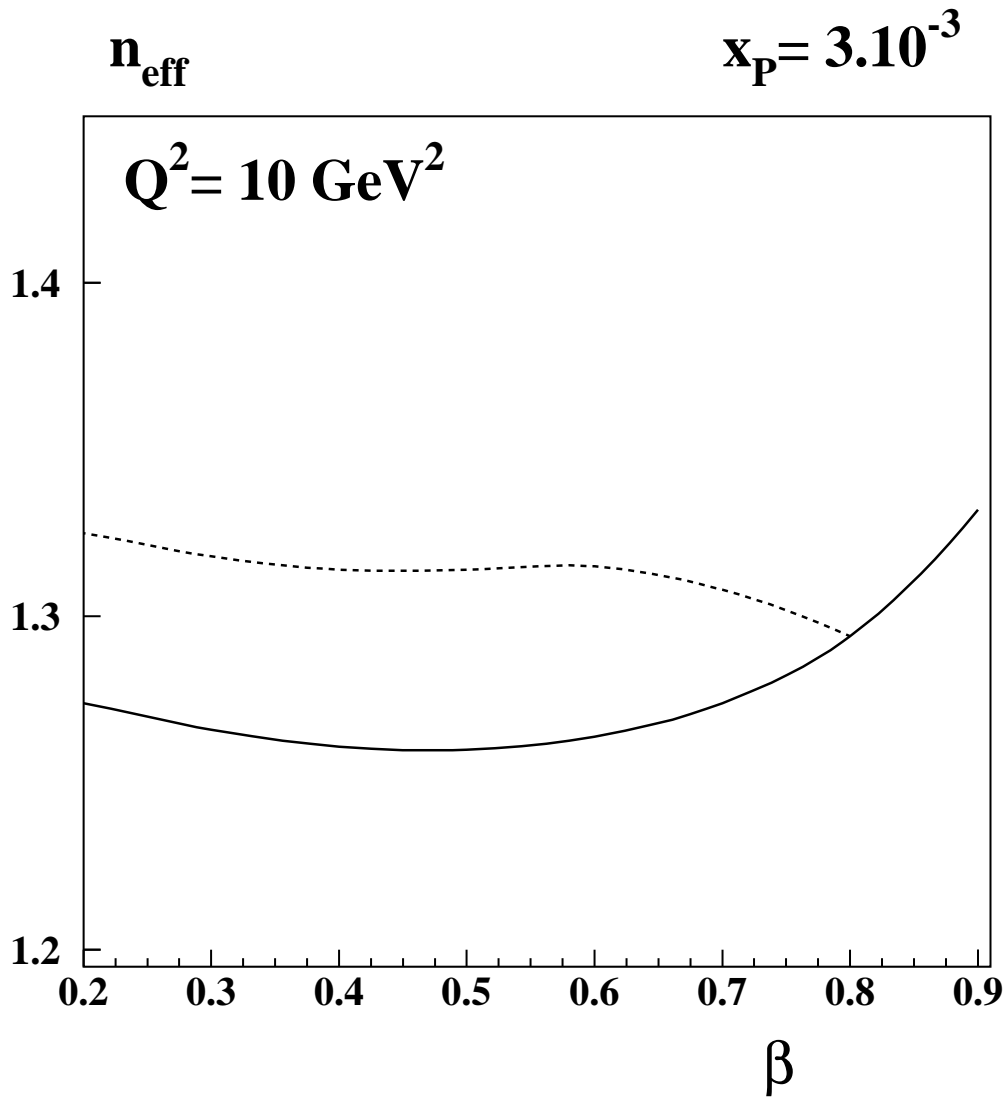
Figure 4: The β dependence of n_{eff} for $x_{\mathbb{P}} = 0.003$ and $Q^2 = 10$ GeV^2. Solid line : (ud) component, dashed line: (ud+cs).
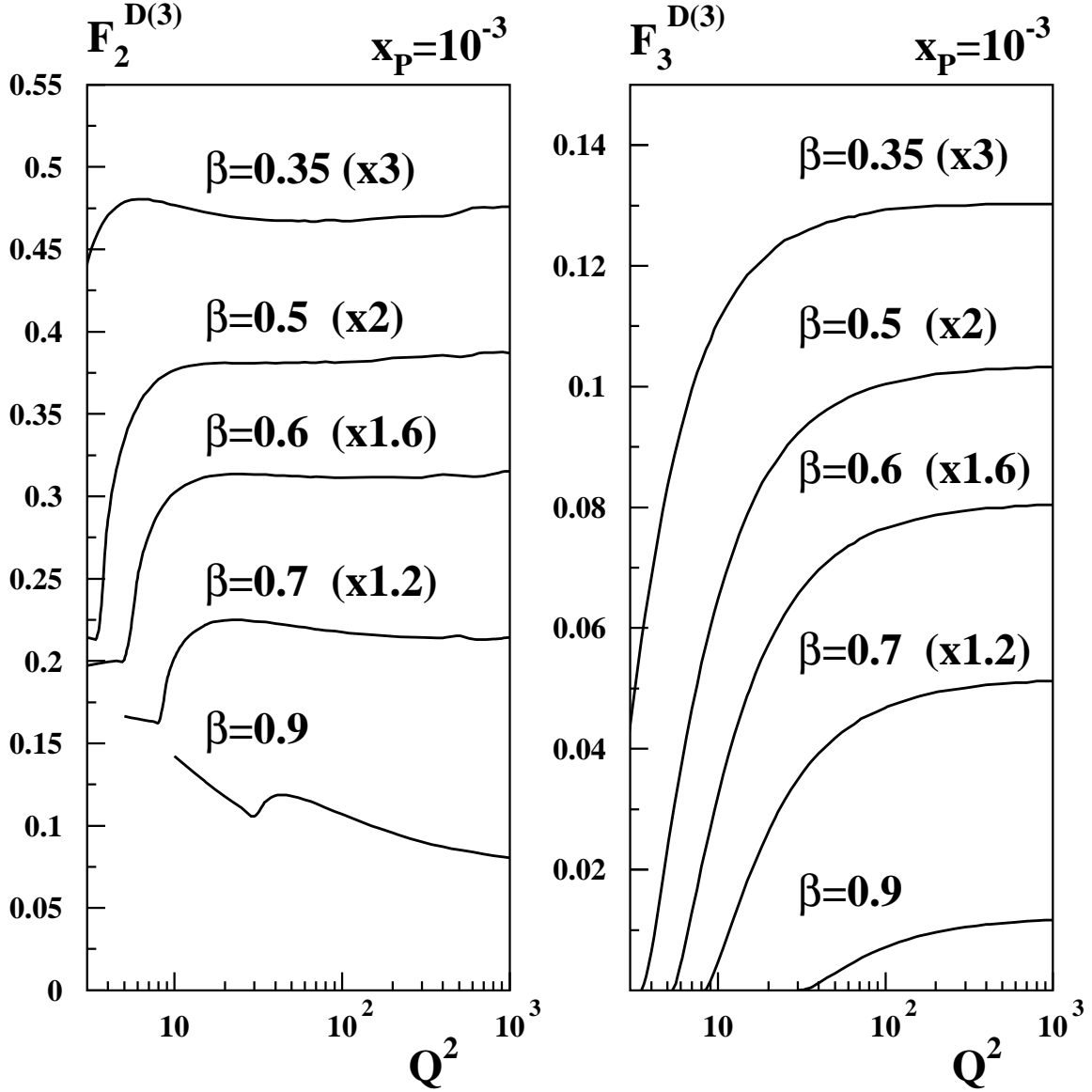
Figure 5: Charm-strange threshold effect in the Q^2 dependence of the diffractive SF $F_2^{D(3)}$ (first box) and on $F_3^{D(3)}$ (second boxe).